Reconstructed Global Total Water Storage Products (1923-2022): Insights and Challenges in Humid and Arid Regions

Jielong Wang[1, 2], Yunzhong Shen[1*], Joseph L. Awange[2], Maryam Tabatabaeiasl[2], Tengfei Feng[1], Ling Yang[1], Yongze Song[3]

[1]College of Surveying and Geo-informatics, Tongji University, Shanghai, 200092, PR China

[2]School of Earth and Planetary Sciences, Spatial Sciences Discipline, Curtin University, Perth, WA, Australia

[3]School of Design and the Built Environment, Curtin University, GPO Box U1987, Perth, WA 6845, Australia

*Corresponding author: Yunzhong Shen (yzshen@tongji.edu.cn)

Key Points:

- A deep learning model for reconstructing global climate-driven total water storage changes is presented for 1923-2022.
- Our reconstruction exhibits superior consistency with GRACE observations compared to GRACE-REC.
- The reconstructed datasets reveal relative reliability and challenges in humid and arid regions.

Abstract

Limited observations of total water storage (TWS) changes derived from the Gravity Recovery and Climate Experiment (GRACE) have impeded our understanding of their full range and long-term variability. In this study, we apply a deep learning model called RecNet to reconstruct global TWS products from 1923 to 2022. RecNet is trained using a novel Weighted Modified Nash-Sutcliffe Efficiency (WMNSE) loss function. Our results reveal that RecNet, trained with WMNSE, yields a more consistent reconstruction than RecNet trained with the commonly-used mean square error loss function. We further show that RecNet achieves superior or comparable performance with four existing global reconstruction datasets and two hydrological models. In addition, these long-term TWS datasets generally exhibit reliable performance in humid regions but pose challenges in arid regions. This study offers alternative centenary TWS change dataset, while highlighting the need for caution when utilizing them in arid regions.

Plain Language Summary

Since 2002, the Gravity Recovery and Climate Experiment (GRACE) and its Follow-On (GRACE-FO) mission, have been keeping a close eye on how much water is being stored in different regions of the world. However, the data collected only covers a relatively short period of about 20 years, which makes it difficult to study long-term changes in water storage. Recently, deep learning methods have shown great promise in helping scientists better understand the Earth's systems. This study uses a deep learning model called RecNet to reconstruct global total water storage (TWS) changes from 1923 to 2022. RecNet is trained using precipitation and temperature as the inputs and GRACE-derived TWS changes as the target. Our results show that RecNet reconstructs the past TWS changes in humid regions, but it has relatively poor performance in arid regions. These findings are also found in existing reconstruction datasets and hydrological models. Therefore, the poor performance is probably attributed to the weak TWS signals in arid regions rather than RecNet itself. This work provides a global reconstruction of centenary TWS changes by the deep learning model. At the same time, it emphasize important considerations for using the long-term TWS datasets in arid regions.

1. Introduction

Since 2002, the Gravity Recovery and Climate Experiment (GRACE) and its Follow-On (GRACE-FO) missions have offered the first observations of total water storage (TWS, the sum of water stored in surface water bodies, snow, soil moisture, and groundwater), which have been extensively used to study global climate changes and variability (Awange et al., 2016; Rodell et al., 2018; Forootan et al., 2019; Tapley et al., 2019; Rodell & Li, 2023), hydrological cycle (Awange et al., 2013; Chen et al., 2020; Rodell & Reager, 2023), and human-induced groundwater depletion (Agutu et al., 2019; Feng et al., 2022; Ali et al., 2024). However, a relatively short record of TWS data (about 20 years) from GRACE and GRACE-FO (referred to as GRACE unless explicitly mentioning GRACE-FO) has hindered our comprehensive analysis of its complete range and long-term variability. While pre-2002 TWS changes can be obtained through hydrological models and in-situ water level measurements (Huang et al., 2013), these methods are unable to provide the same level of accuracy as GRACE because of intrinsic limitations, such as data availability or uncertainty, and difficulties in modeling intricate water storage dynamics (Li et al., 2020, 2021).

Driven by the high demand for long-term TWS data in the scientific community (Huang et al., 2013; Chen et al., 2019), a growing array of studies have been conducted to reconstruct global historical TWS changes (e.g., Table 1). Most recently, Yin et al. (2023) attempted to extend GRACE-derived TWS changes to 1940 by employing different machine learning models (e.g., random forest and neural networks). To evaluate the performance of these models, they randomly split the entire GRACE data into training and testing parts. However, this approach overestimated the models' performance because reconstructing the past TWS data is an extrainterpolation task. The random split strategy incorrectly transformed it into an interpolation task. Deng et al. (2020) produced long-term TWS data using a bias-corrected method to align the reconstruction with the spatiotemporal characteristics of GRACE data, inevitably introducing the issue of reconstructive dependency. Li et al. (2020, 2021) utilized spatiotemporal decomposition techniques to separate the spatial patterns and temporal modes of GRACE TWS, and then reconstructed TWS by establishing relationships between the temporal modes and potential predictors, assuming that the predominant spatial patterns remain constant over time. Subsequently, they selected 26 major river basins of the world to evaluate the reconstructive performance, 'deliberately' focusing on those predominantly distributed in humid climates and ignoring the arid regions.

Both anthropogenic activities and climate variability influence changes in TWS derived from GRACE. Despite distinct predictors having been used in previous studies to build their empirical relationship with GRACE data (e.g., Humphrey & Gudmundsson, 2019; Satish Kumar et al., 2023; Wang et al., 2023), they dominantly present the climatic drivers, as human-induced changes in TWS are not adequately observed and cannot be incorporated into these models. For instance, Humphrey et al. (2016) and Humphrey et al. (2017) indicated that changes in TWS are tightly related to fluctuations in precipitation and temperature and thus can be statistically reconstructed from them. In Humphrey's subsequent study, they used precipitation and temperature data to reconstruct the past climate-driven TWS changes based on a linear water store model (Humphrey & Gudmundsson, 2019), thereby neglecting the potential nonlinear associations between the climatic drivers and TWS changes. Wang et al. (2023) proposed a deep learning model called RecNet to reconstruct centenary TWS changes over the Yangtze River Basin and demonstrated its superior performance than Humphrey and Gudmundsson (2019)'s approach.

In this study, we extend Wang et al. (2023)'s method from a specific basin to a global reconstruction. Specifically, we train RecNet using precipitation, temperature, and GRACE observations to capture the potential nonlinear relationships. Subsequently, we apply the trained network to reconstruct global TWS changes from 1923 to 2022. The reconstructive performance is validated by comparing the results to those of hydrological models and existing reconstruction datasets, with an additional focus on discussing the reliability of these datasets in humid and arid regions.

Table 1. Global reconstructions of GRACE-derived TWS changes

Reference	Method	Data processing	Predictors	Period
Humphrey and Gudmundsson (2019)	Based on a linear water store model	Detrend and deseasonal	Precipitation and temperature	1901-2019
Deng et al. (2020)	Empirical orthogonal function decomposition and linear regression	Separate the polar and non-polar regions	Soil moisture, snow depth, precipitation, temperature, and glacial water mass changes	1981-2020
Li et al. (2020, 2021)	Multiple linear regression, artificial neural network, and autoregressive exogenous model	Detrend and separate the spatial patterns and temporal modes of data	Precipitation, temperature, sea surface temperature, and climate indices	1979-2020
Yin et al. (2023)	Machine learning models	Randomly split the datasets	Hydrological and meteorological variables, land cover, and vegetation indicators	1940-2022
This study	Deep learning model	Detrend and discard the polar regions	Precipitation and temperature	1923-2022

2. Datasets

2.1. Precipitation and temperature data

The monthly precipitation and temperature data are obtained from the Climate Research Unit gridded Time-Series datasets (CRU TS v4.07) at the University of East Anglia, UK (Harris et al., 2020), which provides high-resolution gridded datasets for multiple variables on a 0.5° × 0.5° or finer grid. The data from 2002 to 2022 is used during the model development period, whereas the data from 1923 to 2002 is used for the reconstruction task. We also use the precipitation and temperature data from the Global Land Data Assimilation System (GLDAS) (Beaudoing & Rodell, 2020) to check the robustness of our main results.

2.2. GRACE and GRACE-FO data

The GRACE-derived TWS data from April 2002 to June 2017 and GRACE-FO data from June 2018 to December 2022 are sourced from the Jet Propulsion Laboratory (JPL) Mascons with the Costal Resolution Improvement (CRI) filter. Compared to conventional spherical-harmonic solutions, this dataset is less susceptible to leakage errors and requires few empirical postprocessing steps (Wiese et al., 2019). To verify RecNet's reconstructive capability, the data from April 2008 to December 2022 (70%), from April 2005 to March 2008 (15%), and from April 2002 to March 2005 (15%) are utilized as the training, validation, and testing datasets, respectively. We also test the robustness of the choice of mascon datasets, including CSR (Save et al., 2016) and GSFC mascon solutions (Loomis et al., 2021).

2.3. Auxiliary datasets

To evaluate RecNet's reconstruction, we compare its results with those of GLDAS, and WaterGAP Global Hydrology Model (WGHM) (Müller et al., 2021), and previous studies, including Humphrey and Gudmundsson. (2019) (GRACE-REC), Deng et al. (2020) (Rec-Deng), Li et al. (2020, 2021) (Rec-Li), and Yin et al. (2023) (Rec-Yin) (Table 1). We present key comparison results in the main text, with additional details provided in the supporting information.

3. Methods

RecNet, a lightweight deep learning model, has been successfully applied to reconstruct the past TWS changes over the Yangtze River Basin (Wang et al., 2023). It consists of an encoder path and a decoder path connected through bottleneck layer. The encoder path downsamples the input image, while the decoder path subsequently restores it to its original dimensions (Figure 1a). We refer interested readers to Wang et al. (2023) for further information.

In this study, we apply RecNet to reconstruct global TWS changes from 1923 to 2022 excluding Greenland and Antarctic regions. Considering the water accumulation time-lag effect (Figure S1 and S2), the precipitation and temperature data of current month and previous 11 months are used as inputs, resulting in 24 input channels. A linear trend is removed from GRACE observations, assuming that it is predominantly caused by human factors (Li et al., 2021; Wang et al., 2023). The input and target data are resampled into $1° \times 1°$ grid, and a random crop of 64×64 is used at the training and validation periods. These choices allow RecNet to fit within memory. We show that RecNet is robust to crop sizes like 32×32 and 96×96. We also propose a novel Weighted Modified Nash-Sutcliffe Efficiency (WMNSE) loss function as follows,

$$\mathrm{WMNSE} = \frac{\sum_{i=1}^{n} \omega_i |o_i - p_i|}{\sum_{i=1}^{n} \omega_i |p_i - \overline{p}|} \quad (1)$$

where o and p are the observed and predicted value, respectively; the overbar denotes mean values; n is the number of target data for testing, while ω is the sigmoid weight derived from JPL Mascon data uncertainty, assuming that the higher the uncertainty, the lower the weight. We find that WMNSE exhibits more consistent results than the commonly-used mean square error loss function (Figure 1c). The correlation coefficient (CC) is used to measure the phase consistency between our reconstruction and GRACE observations, and NSE used for phase and amplitude measurements.

$$\mathrm{CC} = \frac{\sum_{t=1}^{n}(o_t-\bar{o})(p_t-\bar{p})}{\sqrt{\sum_{t=1}^{n}(o_t-\bar{o})^2}\sqrt{(p_t-\bar{p})^2}} \tag{2}$$

$$\mathrm{NSE} = 1 - \frac{\sum_{t=1}^{n}(o_t-p_t)^2}{\sum_{t=1}^{n}(p_t-\bar{p})^2} \tag{3}$$

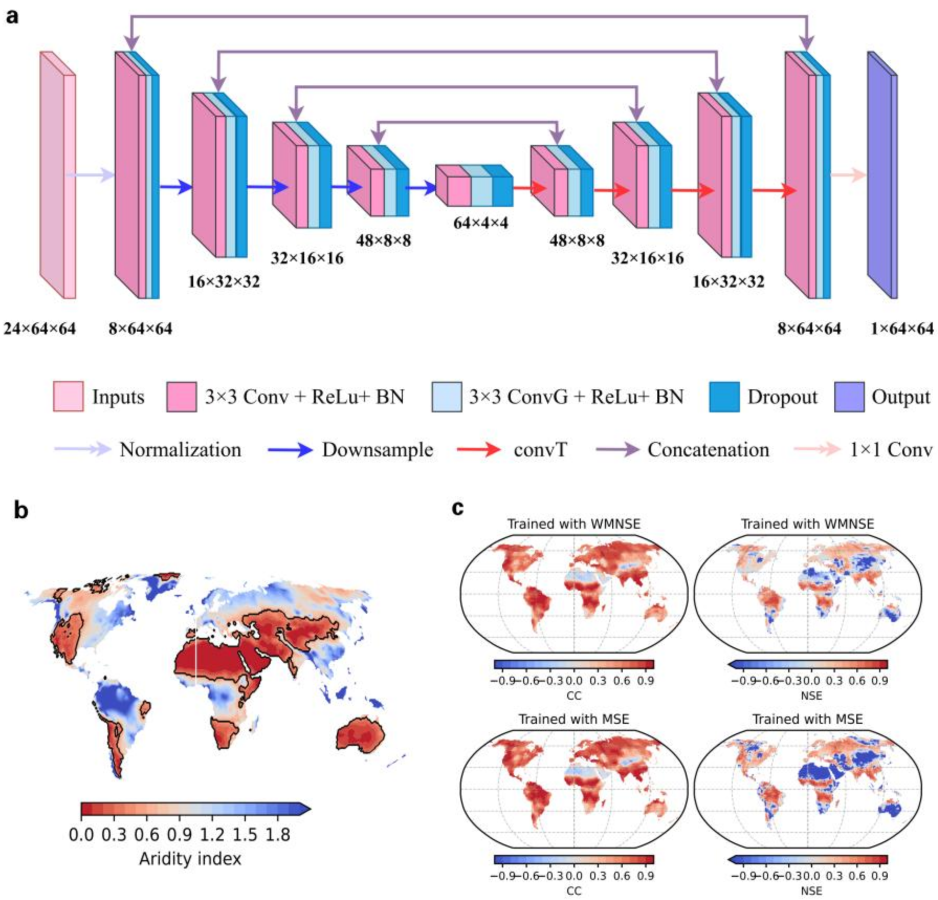

Figure 1. (**a**) The RecNet model architecture. Each box corresponds to a multi-channel feature map. The three numbers around the box denote the feature map's channels, height, and width, respectively. The arrows indicate the different operations performed. Conv for convolution; ConvG, grouped convolution; BN, batch normalization; ConvT, transposed convolution. (**b**) The aridity index with the black contours denotes the arid regions. (**c**) The NSE and CC values between GRACE observations and RecNet trained with WMNSE or MSE during the testing period 2002-2005.

4. Results

4.1. Comparing RecNet's reconstruction with GRACE observations

It is widely recognized that the way the training and testing datasets are split can significantly impact the performance of deep learning models (Medar et al., 2017). Since we focus on reconstructing the past TWS changes, the GRACE data from April 2005 to December 2022 is used as the training (70%) and validation sets (15%), whereas the data from April 2002 to March 2005 (15%) is used as the testing set. As shown in Figure 1c, RecNet achieves satisfactory performance during the testing period in terms of spatial NSE and CC values between its results and GRACE observations. Relatively poor performance is observed in arid regions, where the aridity index, calculated by the ratio between long-term mean precipitation and potential evapotranspiration (Zhang et al., 2019), is less than 0.5 (Figure 1b). In addition, RecNet trained with WMNSE exhibits more consistent performance compared with that trained with MSE. RecNet's performance is also robust to mascon solutions, precipitation and temperature products, and crop sizes (Figure S3).

4.2. Comparing RecNet's reconstruction with GRACE-REC

Compared with Humphrey & Gudmundsson (2019)'s study, RecNet frees us from explicitly building the relationship between the GRACE observations and their climatic drivers. To assess potential benefits from the non-linearity introduced by RecNet, we compute the CC and NSE values between RecNet/GRACE-REC and GRACE data. Since GRACE-REC did not reconstruct the seasonal signals, we apply the seasonal and trend decomposition using the loess (STL) method to deseasonalize the detrended TWS changes (Humphrey et al., 2016). Similar processing is applied to the TWS data derived from GLDAS and WGHM. As for the CC values, all four models reveal comparable performance (Figure 2a, c, e, and g). RecNet, GRACE-REC, and WGHM observe relatively higher performance in humid regions compared to arid regions. However, apparent discrepancies are observed among the four models concerning the NSE values. GRACE-REC reveals negative NSE values across most regions globally, suggesting it probably struggles to reconstruct the amplitude in GRACE-derived TWS changes. WGHM and GLDAS show more positive NSE values compared to GRACE-REC, while notable negative NSE values are observed in many arid regions. Nevertheless, RecNet displays generally positive

NSE values in both arid and humid regions, indicating its better reconstructive performance than GRACE-REC. This is attributed to the introduced non-linearity, as RecNet and GRACE-REC employ the same explanatory variables (i.e., precipitation and temperature). Similar to WGHM and GLDAS, RecNet still observes relatively high NSE values in humid regions compared to arid regions.

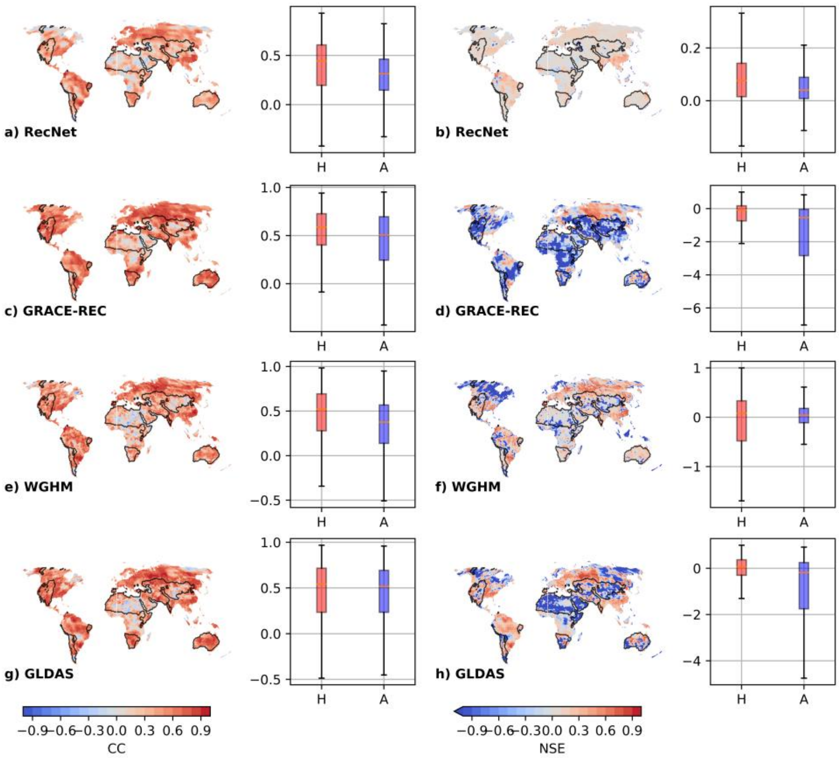

Figure 2. CC and NSE values between GRACE-derived interannual TWS changes with those from RecNet (a-b), GRACE-REC (c-d), WGHM (e-f), and GLDAS (g-h). The box plot to the right summarizes the corresponding metrics in arid (A) and humid (H) regions, respectively.

4.3. Evaluating RecNet's reconstruction in humid and arid regions

We employ the deep ensemble technique to demonstrate the reconstructive reliability of RecNet. Specifically, we train 100 RecNet models, each initialized with different parameters. The ensemble uncertainty is obtained by calculating the variance of predictions made by each model. We also calculate the ensemble NSE between RecNet's reconstruction and GRACE observations during the testing period and empirically categorize RecNet's performance into great ($NSE > 0.6$), satisfactory ($0.25 < NSE \leq 0.6$), good ($0.0 < NSE \leq 0.25$), fair ($-0.25 < NSE \leq 0$), poor ($-0.6 < NSE \leq -0.25$), and bad ($NSE \leq -0.6$). As shown in Figure 3, RecNet exhibits reliable reconstruction in humid regions (e.g., high-latitude areas), whereas its performance is comparatively less satisfactory in arid regions such as Australia. Ensemble NSE values are positive in the humid regions, whereas many arid regions show negative NSE values.

We further compare RecNet's reconstruction with existing long-term TWS changes datasets derived from Rec-Deng, Rec-Li, Rec-Yin, WGHM, and GLDAS over 52 basins in arid regions and 81 basins in humid regions (selected by the area larger than the footprint of GRACE). GRACE-REC is excluded because it only reconstructed the interannual signals. Each dataset is detrended for a fair comparison. Considering the overlapping time coverage, we compare the data from January 1981 to March 2002. The heat map reveals a general consistency among those datasets (Figure 3). Importantly, all exhibit relatively higher CC and NSE values in humid regions compared to arid regions. Three basins in humid regions (Congo, Amazon, and Yangtze) and three in arid regions (Gobi Interior, North Interior in Africa, and Murray-Darling) are shown as example basins. Generally consistent reconstructions are observed in these humid regions, while significant differences are found in the arid regions. In addition, Figure 3 also shows that the reconstructions derived from other datasets align well within the range of uncertainty estimated in our study. These findings indicate that relatively reliable reconstruction can be achieved in humid regions, while significant challenges persist in arid regions.

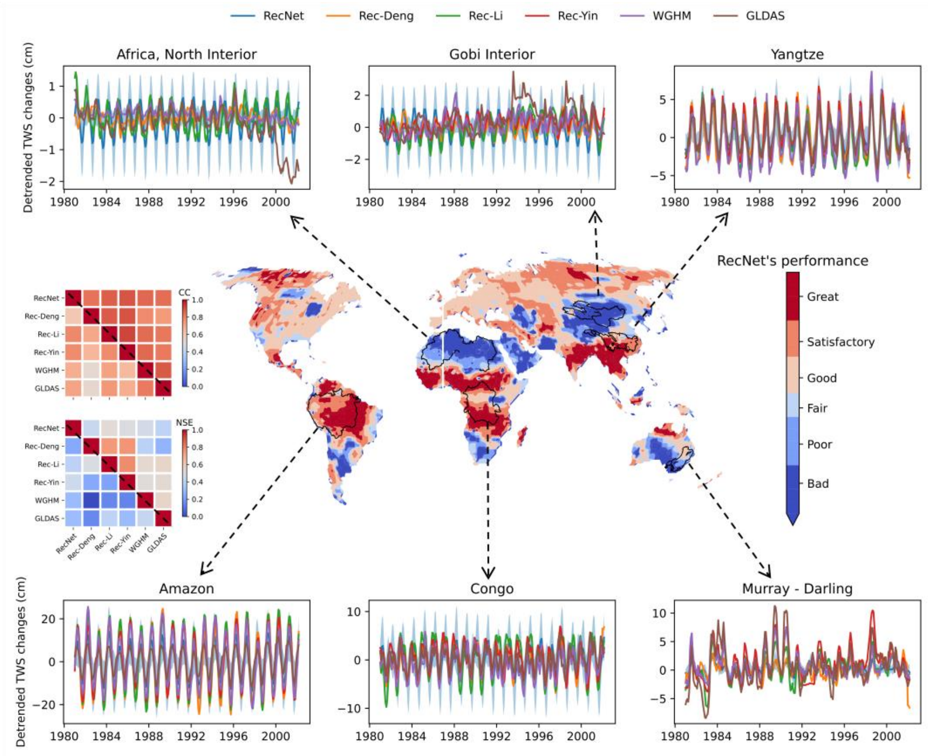

Figure 3. RecNet's reconstruction performance, with showing the comparisons with the detrended TWS changes derived from Rec-Deng, Rec-Li, Rec-Yin, WGHM, and GLDAS in example basins. The light-blue envelope represents the uncertainty ranges of RecNet, which is estimated using deep ensembles. The heat maps in the left side compare RecNet's reconstruction with Rec-Deng/Li/Yin, WGHM, and GLDAS in the 81 basins within humid regions (upper triangle) and 52 basins within the arid regions (lower triangle).

5. Discussions

5.1. Reconstructing long-term trends in TWS changes

GRACE-derived TWS changes represent the combined influence of human activities and climate variability. In the past two decades, apparent TWS trends have been attributed to factors such as groundwater abstraction and the proliferation of reservoirs (Rodell et al., 2018). Previous studies have primarily utilized non-human factors like precipitation and temperature to reconstruct the TWS changes (Li et al., 2021; Yin et al., 2023; Wang et al., 2023). Therefore, human-induced TWS changes may have been under-reconstructed or unreconstructed in these studies due to the absence of long-term observations specifically reflecting human activities. In other words, reconstructed trends in previous studies may have been underestimated or deemed unreliable. Li et al. (2020, 2021) reconstructed the long-term trends using trends estimated from the GRACE period. This approach may be inappropriate given the intensified impacts of human activities in recent years compared to the relatively moderate economic development and wealth levels before 2000. Our study focuses on reconstructing detrended TWS changes driven by precipitation and temperature without detrending these variables. By so doing, we preserve the trends attributed to these climatic variables, as the period before the GRACE era likely experienced predominantly climate-driven TWS changes due to relatively moderate human activities. The possibility of reconstructing the long-term trend will be investigated in our future works. In contrast to Humphrey & Gudmundsson (2019)'s work, which only reconstructed the interannual component, our study simultaneously reconstructs the seasonal signal to provide as comprehensive a range of TWS changes as possible.

5.2. Selection of explanatory variables

Several studies have proposed various models (e.g., linear model, random forest, and neural networks) to reconstruct long-term TWS changes data before GRACE era by learning their empirical relationship with different driving factors (e.g., Humphrey & Gudmundsson, 2019; Satish Kumar et al., 2023; Wang et al., 2023; Yin et al., 2023). For example, Yin et al. (2023) utilized a large set of variables, including land cover, vegetation conditions, and wind speed, to reconstruct the TWS changes, while Li et al. (2020, 2021) utilized precipitation, temperature, sea surface temperature (SST), and climate indices. They found that incorporating climate indices and SST into the reconstruction models can reproduce the ENSO signals. Nevertheless, as depicted in Figure 3, we consistently observe robust results across our reconstruction based solely on precipitation and temperature, as well as other reconstructions utilizing diverse variables and hydrological models. This finding aligns with Humphrey et al. (2016), who indicated that TWS changes can be reconstructed from precipitation and temperature alone. The probable reason for this is that major climate patterns significantly influence precipitation and temperature anomalies, inherently containing information regarding climate patterns. Moreover, changes in TWS are balanced by the rate of precipitation, evapotranspiration, and runoff, where precipitation is the key recharge source for TWS and runoff changes, whereas temperature plays a significant role in influencing evapotranspiration (Chen et al., 2020).

5.3. Reconstructing TWS changes in humid and arid regions

We found better reconstructive performance in humid regions compared to arid ones. This outcome is somewhat anticipated due to the relatively abundant precipitation and TWS changes in humid regions, in contrast to the weak TWS signals in arid regions resulting from limited precipitation and high evapotranspiration. TWS changes in arid regions (e.g., Murray-Darling basin) may have many small and unstable trends caused by irregular precipitation, leading to high uncertainties in these areas (Figure 3). These findings emphasize cautions when applying the reconstructed long-term TWS change datasets (our reconstruction and others) in arid regions. Conversely, the relatively reliable reconstruction in humid regions holds promise for studying long-term TWS changes while discerning the influences of human and natural variability on them. It is important to note that these findings are based on the assumption that GRACE observations serve as the ground truth. Large lakes (e.g., Lake Victoria in Africa), reservoirs, and glaciers may also influence reconstruction, but comprehensively studying their influence is not trivial and will be explored in future with more effort.

6. Conclusions

This study employs RecNet to reconstruct global, excluding the Greenland and Arctic regions, climate-driven TWS changes for 1923-2022. RecNet is trained using precipitation, temperature, GRACE observations, and WMNSE loss function. Our analysis highlights several key findings:

(i) RecNet, when trained with WMNSE, exhibits a more consistent reconstruction than that trained with MSE.

(ii) Despite using only precipitation and temperature data, RecNet demonstrates superior performance over GRACE-REC, which similarly used these two variables to perform the global reconstruction.

(iii) The coherence observed between RecNet's reconstructions and four existing datasets, along with two hydrological models, underscores its efficacy.

(iv) While long-term TWS data, derived from both hydrological models and the reconstruction datasets, exhibit relative reliability in humid regions, their reliability in arid regions is more uncertain. Consequently, caution must be exercised when utilizing these datasets in arid regions.

Acknowledgments

This work was primarily supported by the National Natural Science Foundation of China (Grant No. 42192532 and Grant No. 42274005) and the China Scholarship Council (Grant No. 202306260241).

Open Research

All the data used in this study are available online: CSR mascons data (https://www2.csr.utexas.edu/grace/RL06_mascons.html); GSFC mascons data (https://earth.gsfc.nasa.gov/geo/data/grace-mascons); JPL mascons data (https://grace.jpl.nasa.gov/data/get-data/jpl_global_mascons/); GLDAS (https://disc.gsfc.nasa.gov/datasets?keywords=GLDAS); CRU TS (https://www.uea.ac.uk/web/groups-and-centres/climatic-research-unit/data); GRACE-REC (https://figshare.com/articles/dataset/GRACE-REC_A_reconstruction_of_climate-driven_water_storage_changes_over_the_last_century/7670849); Rec-Deng (https://www.geodoi.ac.cn/WebEn/doi.aspx?Id=3226); Rec-Li (https://datadryad.org/stash/dataset/doi:10.5061/dryad.z612jm6bt); WGHM (https://doi.pangaea.de/10.1594/PANGAEA.948461?format=html#download). Maps are created through Cartopy version 0.21.0 (https://doi.org/10.5281/zenodo.1182735; Elson et al., 2021). Python code used for this work and the reconstructed data by RecNet are published at Zenodo. https://doi.org/10.5281/zenodo.10695487 (Wang, 2024).

References

Agutu, N. O., Awange, J. L., Ndehedehe, C., Kirimi, F., & Kuhn, M. (2019). GRACE-derived groundwater changes over Greater Horn of Africa: Temporal variability and the potential for irrigated agriculture. Science of the Total Environment, 693, 133467. https://doi.org/10.1016/j.scitotenv.2019.07.273

Ali, S., Ran, J., Luan, Y., Khorrami, B., Xiao, Y., & Tangdamrongsub, N. (2024). The GWR model-based regional downscaling of GRACE/GRACE-FO derived groundwater storage to investigate local-scale variations in the North China Plain. Science of the Total Environment, 908(October 2023), 168239. https://doi.org/10.1016/j.scitotenv.2023.168239

Awange, J. L., Anyah, R., Agola, N., Forootan, E., & Omondi, P. (2013). Potential impacts of climate and environmental change on the stored water of Lake Victoria Basin and economic implications. Water Resources Research, 49(12), 8160–8173. https://doi.org/10.1002/2013WR014350

Awange, J. L., Khandu, Schumacher, M., Forootan, E., & Heck, B. (2016). Exploring hydro-meteorological drought patterns over the Greater Horn of Africa (1979-2014) using remote sensing and reanalysis products. Advances in Water Resources, 94, 45–59.

https://doi.org/10.1016/j.advwatres.2016.04.005
Beaudoing, H., & Rodell, M. NASA/GSFC/HSL (2020), GLDAS Noah Land Surface Model L4 monthly 0.25 x 0.25 degree V2.1, Greenbelt, Maryland, USA, Goddard Earth Sciences Data and Information Services Center (GES DISC) [Dataset], Accessed: [2023-01-07], https://doi.org/10.5067/SXAVCZFAQLNO
Chen, H., Zhang, W., Nie, N., & Guo, Y. (2019). Long-term groundwater storage variations estimated in the Songhua River Basin by using GRACE products, land surface models, and in-situ observations. Science of the Total Environment, 649, 372–387. https://doi.org/10.1016/j.scitotenv.2018.08.352
Chen, J., Tapley, B., Rodell, M., Seo, K. W., Wilson, C., Scanlon, B. R., & Pokhrel, Y. (2020). Basin-Scale River Runoff Estimation From GRACE Gravity Satellites, Climate Models, and In Situ Observations: A Case Study in the Amazon Basin. Water Resources Research, 56(10), 1–21. https://doi.org/10.1029/2020WR028032
Deng, S., Liu, S., & Mo, X. (2020). Assessment of three common methods for estimating terrestrial water storage change with three reanalysis datasets. Journal of Climate, 33(2), 511–525. https://doi.org/10.1175/JCLI-D-18-0637.1
Elson, P., Sales de Andrade, E., Lucas, G., May, R., Hattersley, R., Campbell, E., Dawson, A., Raynaud, S., scmc72, Little, B., Snow, A. D., Donkers, K., Blay, B., Killick, P., Wilson, N., Peglar, P., lbdreyer, Andrew, Szymaniak, J., Berchet, A., Bosley, C., Davis, L., Filipe, Krasting, J., Bradbury, M., Kirkham, D., stephenworsley, Clément, Caria, G., & Hedley, M.: SciTools/cartopy: v0.21.0, Zenodo [Code], https://doi.org/10.5281/zenodo.1182735, 2021.
Forootan, E., Khaki, M., Schumacher, M., Wulfmeyer, V., Mehrnegar, N., van Dijk, A. I. J. M., Brocca, L., Farzaneh, S., Akinluyi, F., Ramillien, G., Shum, C. K., Awange, J., & Mostafaie, A. (2019). Understanding the global hydrological droughts of 2003–2016 and their relationships with teleconnections. Science of the Total Environment, 650(September 2018), 2587–2604. https://doi.org/10.1016/j.scitotenv.2018.09.231
Feng, T., Shen, Y., Chen, Q., Wang, F., & Zhang, X. (2022). Groundwater storage change and driving factor analysis in north china using independent component decomposition. Journal of Hydrology, 609(July 2021), 127708. https://doi.org/10.1016/j.jhydrol.2022.127708
Harris, I., Osborn, T. J., Jones, P., & Lister, D. (2020). Version 4 of the CRU TS monthly high-resolution gridded multivariate climate dataset. Scientific Data, 7(1), 1–18. https://doi.org/10.1038/s41597-020-0453-3
Huang, Y., Salama, M. S., Krol, M. S., Van Der Velde, R., Hoekstra, A. Y., Zhou, Y., & Su, Z. (2013). Analysis of long-term terrestrial water storage variations in the Yangtze River basin. Hydrology and Earth System Sciences, 17(5), 1985–2000. https://doi.org/10.5194/hess-17-1985-2013
Humphrey, V., & Gudmundsson, L. (2019). GRACE-REC: A reconstruction of climate-driven water storage changes over the last century. Earth System Science Data, 11(3), 1153–1170.

https://doi.org/10.5194/essd-11-1153-2019

Humphrey, V., Gudmundsson, L., & Seneviratne, S. I. (2016). Assessing Global Water Storage Variability from GRACE: Trends, Seasonal Cycle, Subseasonal Anomalies and Extremes. Surveys in Geophysics, 37(2), 357–395. https://doi.org/10.1007/s10712-016-9367-1

Humphrey, V., Gudmundsson, L., & Seneviratne, S. I. (2017). A global reconstruction of climate-driven subdecadal water storage variability. Geophysical Research Letters, 44(5), 2300–2309. https://doi.org/10.1002/2017GL072564

Li, F., Kusche, J., Chao, N., Wang, Z., & Löcher, A. (2021). Long-Term (1979-Present) Total Water Storage Anomalies Over the Global Land Derived by Reconstructing GRACE Data. Geophysical Research Letters, 48(8), 1–10. https://doi.org/10.1029/2021GL093492

Li, F., Kusche, J., Rietbroek, R., Wang, Z., Forootan, E., Schulze, K., & Lück, C. (2020). Comparison of data-driven techniques to reconstruct (1992–2002) and predict (2017–2018) GRACE-like gridded total water storage changes using climate inputs. Water Resources Research, 56(5). https://doi.org/10.1029/2019WR026551

Loomis, B. D., D. Felikson, T. J. Sabaka, & B. Medley (2021). High-spatial-resolution mass rates from GRACE and GRACE-FO: Global and ice sheet analyses. Journal of Geophysical Research: Solid Earth, https://doi.org/10.1029/2021JB023024

Medar, R., Rajpurohit, V. S., & Rashmi, B. (2017). Impact of Training and Testing Data Splits on Accuracy of Time Series Forecasting in Machine Learning. 2017 International Conference on Computing, Communication, Control and Automation, ICCUBEA 2017, 1–6. https://doi.org/10.1109/ICCUBEA.2017.8463779

Müller Schmied, H., Caceres, D., Eisner, S., Flörke, M., Herbert, C., Niemann, C., Asali Peiris, T., Popat, E., Theodor Portmann, F., Reinecke, R., Schumacher, M., Shadkam, S., Telteu, C. E., Trautmann, T., & Döll, P. (2021). The global water resources and use model WaterGAP v2.2d: Model description and evaluation. Geoscientific Model Development, 14(2), 1037–1079. https://doi.org/10.5194/gmd-14-1037-2021

Rodell, M., Famiglietti, J. S., Wiese, D. N., Reager, J. T., Beaudoing, H. K., Landerer, F. W., & Lo, M. H. (2018). Emerging trends in global freshwater availability. Nature, 557(7707), 651–659. https://doi.org/10.1038/s41586-018-0123-1

Rodell, M., & Li, B. (2023). Changing intensity of hydroclimatic extreme events revealed by GRACE and GRACE-FO. Nature Water, 1(3), 241–248. https://doi.org/10.1038/s44221-023-00040-5

Rodell, M., & Reager, J. T. (2023). Water cycle science enabled by the GRACE and GRACE-FO satellite missions. Nature Water, 1(1), 47–59. https://doi.org/10.1038/s44221-022-00005-0

Satish Kumar, K., AnandRaj, P., Sreelatha, K., & Sridhar, V. (2023). Reconstruction of GRACE terrestrial water storage anomalies using Multi-Layer Perceptrons for South Indian River basins. Science of the Total Environment, 857(October 2022), 159289. https://doi.org/10.1016/j.scitotenv.2022.159289

Save, H., Bettadpur, S., & Tapley, B. D. (2016). High-resolution CSR GRACE RL05 mascons. Journal of Geophysical Research: Solid Earth, 121(10), 7547-7569. https://doi.org/10.1002/2016JB013007

Tapley, B. D., Watkins, M. M., Flechtner, F., Reigber, C., Bettadpur, S., Rodell, M., Sasgen, I., Famiglietti, J. S., Landerer, F. W., Chambers, D. P., Reager, J. T., Gardner, A. S., Save, H., Ivins, E. R., Swenson, S. C., Boening, C., Dahle, C., Wiese, D. N., Dobslaw, H., … Velicogna, I. (2019). Contributions of GRACE to understanding climate change. Nature Climate Change, 9(5), 358–369. https://doi.org/10.1038/s41558-019-0456-2

Wang, J. (2024). A global reconstruction of climate-driven total water storage changes using RecNet. Zenodo. https://doi.org/10.5281/zenodo.10695487

Wang, J., Shen, Y., Awange, J. L., & Yang, L. (2023). A deep learning model for reconstructing centenary water storage changes in the Yangtze River Basin. Science of the Total Environment, 905(August), 167030. https://doi.org/10.1016/j.scitotenv.2023.167030

Wiese, D. N., Yuan, D. N., Boening, C., Landerer, F. W., & Watkins, M. M. (2019). JPL GRACE Mascon Ocean, Ice, and Hydrology Equivalent Water Height RL06 CRI Filtered Version 02. Ver. 02. PO.DAAC, CA, USA. [Dataset] accessed [2023-01-06] at https://doi.org/10.5067/TEMSC-3JC62

Yin, J., Slater, L. J., Khouakhi, A., Yu, L., Liu, P., Li, F., Pokhrel, Y., & Gentine, P. (2023). GTWS-MLrec: global terrestrial water storage reconstruction by machine learning from 1940 to present. Earth System Science Data, 15(12), 5597–5615. https://doi.org/10.5194/essd-15-5597-2023

Zhang, Y., He, B., Guo, L., Liu, J., & Xie, X. (2019). The relative contributions of precipitation, evapotranspiration, and runoff to terrestrial water storage changes across 168 river basins. Journal of Hydrology, 579(September), 124194. https://doi.org/10.1016/j.jhydrol.2019.124194